

Forum Original Research Communication

Reversible Modulation of Cell Cycle Kinetics in NIH/3T3 Mouse Fibroblasts by Inducible Overexpression of Mitochondrial Manganese Superoxide Dismutase

AEKYONG KIM,¹ WEIXIONG ZHONG,^{2,3} and TERRY D. OBERLEY^{2,3}

ABSTRACT

To study the mechanism(s) by which manganese-containing superoxide dismutase (MnSOD) mediates cellular growth inhibition, an inducible retroviral vector system regulated by the *lac* repressor was used to overexpress MnSOD protein in NIH/3T3 cells. Increased MnSOD activity led to decreased cell growth due to prolonged cell cycle transition times in G₁ and S phases without significant changes in G₂/M phase. Changes in cell cycle transition time were reversible and tightly correlated with MnSOD levels. A transient increase of reactive oxygen species and concomitant decrease in mitochondrial membrane potential were documented following MnSOD induction. *N*-Acetyl-L-cysteine prevented growth inhibition by MnSOD. Our data suggest that MnSOD may serve a physiological function of regulating cell cycle progression through its prooxidant activity of generating hydrogen peroxide, resulting in coordination of mitochondrial redox state and cellular proliferation. *Antioxid. Redox Signal.* 6, 489–500.

INTRODUCTION

SUPEROXIDE DISMUTASES (SODs; EC 1.15.1.1) catalyze the dismutation of superoxide anion (O₂^{•-}) to oxygen (O₂) and hydrogen peroxide (H₂O₂) through the completion of a reduction/oxidation cycle involving active-site metal catalysis. In eukaryotic cells, three isoforms of SOD have been identified: extracellular copper- and zinc-containing SOD (ECSOD), mitochondrial manganese-containing SOD (MnSOD), and cytoplasmic/nuclear copper- and zinc-containing SOD (CuZnSOD). Although these enzymes serve as antioxidant enzymes (AOEs) under oxidative stress condition, SODs are also intimately involved in the regulation of cell behavior. For example, ECSOD activity inversely correlated with telomere shortening in human fibroblasts (27), and abnormal CuZnSOD structure in humans is strongly implicated in the development of amyotrophic lateral sclerosis (29). MnSOD activity *in vivo* is often down-regulated in cancer cells compared with adjacent normal cells, and an in-

verse correlation between MnSOD activity and cellular growth potential has been well documented in both cancer and nonmalignant cells (20).

Mitochondria are known to produce O₂^{•-} at the rate of 1–2% of O₂ consumed during oxidative phosphorylation and electron transfer (19). MnSOD ensures the efficient removal of mitochondrial O₂^{•-} and protects mitochondria from oxidative damage by O₂^{•-}. MnSOD expression is crucial for survival because MnSOD null mice exhibit neonatal lethality, and CuZnSOD fails to compensate for MnSOD deficiency (6). There are other endogenous sources of reactive oxygen species (ROS) besides mitochondria. For example, the mitogenic oxidase Nox1 located at the plasma membrane generates O₂^{•-}, which is secondarily converted to H₂O₂. When overexpressed, Nox1 enhanced proliferation and tumorigenicity in nonmalignant cells (2).

Under oxidative stress conditions, a battery of genes, often classified as phase II detoxifying genes, are up-regulated as a

¹Molecular and Environmental Toxicology Center, ²Department of Pathology and Laboratory Medicine, University of Wisconsin, Medical School, Madison, WI.

³Pathology and Laboratory Medicine Service, William S. Middleton Veterans Memorial Hospital, Madison, WI.

protective adaptive response to electrophiles and ROS, and this response is often mediated through the activation of an antioxidant response element (ARE). However, unlike other AOE that produce nonreactive end products, SODs convert $O_2^{\cdot-}$ into H_2O_2 with a reduction potential of 1,060 E°/mV, which therefore results in the production of a second oxidant (4). Without sufficient antioxidants or AOE activities to further remove H_2O_2 , elevated SOD activity alone may lead to subcellular accumulation of H_2O_2 and establish a transient oxidative environment. Therefore, SODs may serve as an AOE only when H_2O_2 -removing capacity is adequate, which can be accomplished by increasing glutathione concentration, catalase, or glutathione peroxidase (GPx) activity (30). Although ARE is one of the *cis*-regulatory elements in the promoter region of *sod2* (MnSOD gene) (8), it is yet to be determined whether MnSOD induction under oxidative stress is achieved by ARE activation.

Whereas an antioxidant function of MnSOD is well accepted, the possible effects of a prooxidant activity of MnSOD due to its production of H_2O_2 are more controversial. It has been demonstrated that when MnSOD-overexpressing cells were challenged with additional oxidative stressors, elevated MnSOD levels were often associated with increased viability and decreased apoptosis (3, 12). However, another article in this issue (23) demonstrated that skin keratinocytes from MnSOD-overexpressing transgenic mice had more apoptosis than those from wild-type mice after exposure to a single dose of a carcinogenic initiator followed by a single dose of phorbol ester. Elevated MnSOD may have potentiated phorbol ester-induced apoptosis through its prooxidant activity.

Studies of MnSOD-overexpressing clones developed from malignant and nonmalignant cell lines demonstrated that elevated MnSOD activity led to increased steady-state levels of ROS, with resultant inhibition of cell growth (15–17, 25). Simultaneous overexpression of catalase, both mitochondrial and cytosolic forms, was able to reverse growth inhibition by overexpressed MnSOD. Enhanced mitochondrial functions were documented upon simultaneous overexpression with MnSOD and catalase compared with MnSOD alone (25). These observations led us to postulate that cells actively regulate MnSOD expression under normal physiological conditions and that MnSOD prooxidant activity of producing H_2O_2 is utilized to modulate mitochondrial function with resultant effects on cell physiology.

In this study, we used an inducible retroviral vector system regulated by *lac* repressor to investigate the effects of elevated MnSOD activity on cell growth and cell cycle progression. We demonstrate that inducible MnSOD expression occurred in inducer dose-dependent and induction time-dependent manners. Correct subcellular localization of induced MnSOD and its elevated activity were confirmed by immunogold electron microscopy (EM) and MnSOD activity assay, respectively. Decreased cell growth occurred following induction of MnSOD. Modulation of cell cycle kinetics by MnSOD was transient and reversible, and transient cellular redox changes preceded cell cycle kinetic changes mediated by overexpressed MnSOD. Taken together, these findings indicate that, under physiological conditions, the prooxidant activity of MnSOD is used to modulate cell cycle progression and cell growth.

MATERIALS AND METHODS

Chemicals and reagents

All chemicals were purchased from Sigma Chemical Co. (St. Louis, MO, U.S.A.), unless otherwise specified. MDCK (canine normal kidney epithelial cell line) cells were obtained from the American Type Culture Collection (Manassas, VA, U.S.A.). Tissue culture supplies were from Falcon (Becton–Dickinson Labware, Franklin Lakes, NJ, U.S.A.). Dulbecco's modified Eagle medium (DMEM) with high glucose (4.5 g/L), Geneticin (G418), isopropyl β -thiogalactoside (IPTG), and LipofectAMINE were obtained from Life Technology Inc. (Gaithersburg, MD, U.S.A.). Fetal bovine serum was purchased from HyClone (Logan, UT, U.S.A.). 5,5',6,6'-Tetrachloro-1,1',3,3'-tetraethylbenzimidazolyl carbocyanine iodide (JC-1), 5-(and-6)-carboxy-2',7'-dichlorofluorescein diacetate (CDCFDA), and 2',7'-dichlorofluorescein diacetate (H_2 DCFDA) were obtained from Molecular Probes (Eugene, OR, U.S.A.). 3'SS1 cells and LNXCO3 retroviral vectors were kind gifts from Dr. Igor B. Roninson at the University of Illinois (Chicago, IL, U.S.A.). Human MnSOD cDNA (pcDNA3.1/*hsod2* plasmid) and primary antibody against human MnSOD were generously provided by Dr. Larry W. Oberley of the University of Iowa (Iowa City, IA, U.S.A.).

Cell culture

Cells were routinely maintained in T75 flasks at 25–90% confluency in DMEM with 10% serum at 37°C in a humidified atmosphere of 95% air and 5% CO_2 . Media were renewed every 3–4 days. Trypsin at 0.05% and 0.53 mM EDTA were used for routine subculture. Cells with < a passage number of 30 were used in all experiments. Mycoplasma contamination was regularly tested using Immun-Mark Mycotest kit (ICN Biomedicals Inc., Aurora, OH, U.S.A.), and was negative in the cultures used for these studies.

*Construction of LNXCO3/*hsod2* vector*

Detailed information regarding the LNXCO3 retroviral vector utilized in this study is available elsewhere (5). Human MnSOD with isoleucine at amino acid position 58 was shown to have higher enzyme activity (twofold) compared with MnSOD with threonine at the same position (32). Human MnSOD cDNA with Ile⁵⁸ was cloned into the LNXCO3 vector linearized by *Bgl*III and *Not*I digestion. The LNXCO3/*hsod2* construct was sequenced to confirm the orientation and the absence of mutations in the coding sequence of human MnSOD cDNA (analysis performed by the Biotechnology Center, University of Wisconsin).

Stable transfection and clonal selection

The 3'SS1 cells were developed from NIH/3T3 cells by stable transfection of the p3'SS plasmid (Stratagene, La Jolla, CA, U.S.A.) from which *lac* repressor proteins are constitutively expressed (5). Stable transfection of the LNXCO3/*hsod2* construct into 3'SS1 cells was performed using LipofectAMINE according to the manufacturer's recommendation. After 48 h, cells were subcultured and selected with 800 μ g/ml G418 for 15 days. Multiple clones were selected and screened

for inducibility of MnSOD immunoreactive protein by 10 $\mu\text{g/ml}$ IPTG at 48 h after induction. The best clone (hms1-clone) with low background and high inducible MnSOD expression was chosen for the studies reported herein.

Immunogold EM

Cells were fixed in Carson-Millonig's fixative and rinsed with Sorenson's buffer (pH 7.4). Detailed procedures are available elsewhere (32). Cells were labeled with anti-human MnSOD antibody and gold-conjugated secondary antibody (15 nm gold-conjugated goat anti-rabbit IgH+L; BB International, Cardiff, U.K.). Grids were observed and photographed with an electron microscope (Hitachi H-600). Micrographs of at least 30 cells per experimental condition were randomly taken. The area of mitochondria and the density of immunogold beads in randomly selected cells were quantitatively analyzed by image analysis software (Scion Image Beta 4.02, Scion Corp., Frederick, MD, U.S.A.).

MnSOD activity assay

Cells were washed and scrape-harvested in phosphate-buffered saline (PBS). Cell pellets were resuspended in 50 mM potassium phosphate buffer (pH 7.8) and sonicated at 4°C for 1 min under the following conditions: a sonic dismembrator (Fisher Scientific Model 550, Fisher Scientific, Pittsburgh, PA, U.S.A.) was equipped with a cup horn filled with ice-cold water (Branson Ultrasonic Corp., Danbury, CT, U.S.A.), and amplitude was placed at setting 5. Total protein concentration was measured using the Bradford assay (Bio-Rad Laboratories, Hercules, CA, U.S.A.). Samples were kept at -70°C . On the day of assay, samples were thawed and resonicated for 10 s using the same conditions described above. SOD activity was measured using the nitro blue tetrazolium (NBT) assay (15).

Western blotting

Cells were washed and scrape-harvested in PBS. Whole-cell lysates were prepared with M-PER mammalian protein extraction reagent (Pierce, Rockford, IL, U.S.A.). Samples were centrifuged at 18,845 g for 15 min at 4°C, and total protein concentration of supernatant was measured as described above. Ten micrograms of total proteins was separated and transferred to a nitrocellulose membrane using standard sodium dodecyl sulfate-polyacrylamide gel electrophoresis procedure. Membranes were blocked in 5% nonfat milk in TBST (153 mM Tris-HCl, 150 mM NaCl, and 0.05% Tween 20, pH 7.8). After anti-MnSOD antibody (1:5,000 dilution) and horseradish peroxidase-conjugated secondary antibody (1:10,000 dilution) (Bio-Rad Laboratories) incubations, signals were detected using ECL plus and Storm 860 and quantitated using ImageQuant software version 5.0 (Amersham Bioscience Corp., Piscataway, NJ, U.S.A.). Either anti- β -actin (1:100,000 dilution) (Sigma) or anti-glyceraldehyde-3-phosphate dehydrogenase (GAPDH) (1:100,000 dilution) (Advanced Immuno Chemical Inc., Long Beach, CA, U.S.A.) antibody was used to normalize MnSOD signals. Anti-MnSOD antibody used in current studies was shown to detect both human and murine MnSOD proteins (15, 16).

Growth curve and population doubling time

Cells were seeded at 2×10^5 per 10-cm dish and cultured for 48 h to insure recovery from the plating process and to reach log phase before the initiation of induction. Cells were treated with 25 $\mu\text{g/ml}$ IPTG in 10 ml of fresh medium. Every 24 h, cells were trypsinized and counted using a Coulter particle counter (Coulter Corp., Miami, FL, U.S.A.). Population doubling time (T_d) was calculated from growth curves using the formula $T_d = 0.693t/\ln(N_t/N_0)$, where t is the time in hours, N_t is the cell number at time t , and N_0 is the cell number at the initial time.

Cell cycle kinetic measurements

Cells were seeded at 2×10^5 per 10-cm dish and cultured for 48 h. MnSOD induction was initiated with 25 $\mu\text{g/ml}$ IPTG in 10 ml of fresh medium at 0 h. After a given induction time, cells were pulsed for 30 min with 20 μM bromodeoxyuridine (BrdU) [BrdU pulse period], and cell cycle progression was allowed to proceed for 5 h in fresh medium [5 h-chase period]. At the end of a 5-h chase period, cells were fixed with 95% ethanol and stained for BrdU incorporation and DNA content (31). In results, time-course studies are described as the time of induction with actual times analyzed being 5.5 h longer as necessary for pulse and chase analysis. Flow cytometry analysis was performed using a FACSCalibur flow cytometer (BD Bioscience, San Jose, CA, U.S.A.); a minimum of 10,000 events was collected for analysis. Potential doubling time (T_{pot}), S phase transition time (T_S), and G_2/M phase transition time ($T_{G2/M}$) were calculated according to equations developed previously (31); G_1 phase transition time (T_{G1}) was calculated by subtracting T_S and $T_{G2/M}$ from T_{pot} .

Cell sorting and cell cycle analysis

Cells were harvested using cell dissociation solution (Sigma) and stained with 10 $\mu\text{g/ml}$ Hoechst 33342 (Molecular Probes, H1399) at 37°C for 30 min. Live cells in G_1 phase were sorted according to Hoechst DNA profile using a FACS Vantage SE flow cytometer (BD Bioscience). Twelve hours after replating at 5×10^5 cells per 60-mm dish, cells were pulsed with 20 μM BrdU for 30 min and fixed with 95% ethanol. Staining and analysis for BrdU incorporation and DNA content were performed as described above. Cells in each cell cycle phase were expressed as a percentage of the gated population.

Intracellular ROS and mitochondrial membrane potential measurements

Detailed methods were described previously (17). Cells were harvested using cell dissociation solution (Sigma) and resuspended at 1×10^6 cells/ml in fresh medium containing 10 μM H_2DCFDA for intracellular ROS or 1 μM JC-1 for mitochondrial membrane potential, respectively. CDCFDA at 10 μM was used to normalize uptake, efflux, and ester cleavage of H_2DCFDA . After staining for 30 min at 37°C, 5 $\mu\text{g/ml}$ propidium iodide (PI) was added, and analysis was performed using a FACSCalibur flow cytometer (BD Bioscience). A minimum of 10,000 events was collected for analysis of the geometric mean fluorescence of each dye in live cells.

DNA fluorometric assay

Detailed procedures are described elsewhere (24). Cells were washed twice with Krebs–Ringer buffer (KR buffer, pH 7.4) (Sigma) and frozen at -70°C in 100 μl of KR buffer per well overnight. On the day of assay, plates were thawed at room temperature for at least 2 h. Two hundred microliters of TNE high-salt solution (10 mM Tris base, 1 mM EDTA•2Na, 2 M NaCl, pH 7.4) containing 10 $\mu\text{g}/\text{ml}$ Hoechst 33258 (Sigma) was added to each well. Plates were incubated at least 2 h at room temperature before measurement of Hoechst fluorescence in each well at excitation wavelength of 352 nm and emission wavelength of 461 nm. KR buffer was used as a blank, and Hoechst fluorescence from media was subtracted as background.

Statistics

Statistical analysis was performed using either Student's paired *t* test with one-tailed distribution or one-way ANOVA for comparison of different groups.

RESULTS

Inducible MnSOD overexpression in NIH/3T3 cells

IPTG is a synthetic analogue of β -galactoside, which is a natural inducer for the *lac* operon in *Escherichia coli*, regulating the transcription of genes for lactose metabolism (14). Unlike other inducers used in inducible gene expression systems, IPTG is metabolically inert. Therefore, IPTG is a reasonable choice of inducer for our study, which concerns cellular ROS levels and redox capacity of cells. We tested the effects of IPTG on cellular ROS levels using H_2DCFDA and flow cytometry and found no significant changes in intracellular ROS levels over a 72-h time period with up to 100 $\mu\text{g}/\text{ml}$ concentration of IPTG in parental NIH/3T3 cells (data not shown).

As shown in Fig. 1A and B, immunoreactive MnSOD protein was increased at 48 h in an IPTG dose-dependent manner with a maximum of 2.7-fold increase at 25 $\mu\text{g}/\text{ml}$ IPTG treatment in hms1-clone cells. Interestingly, there were decreases

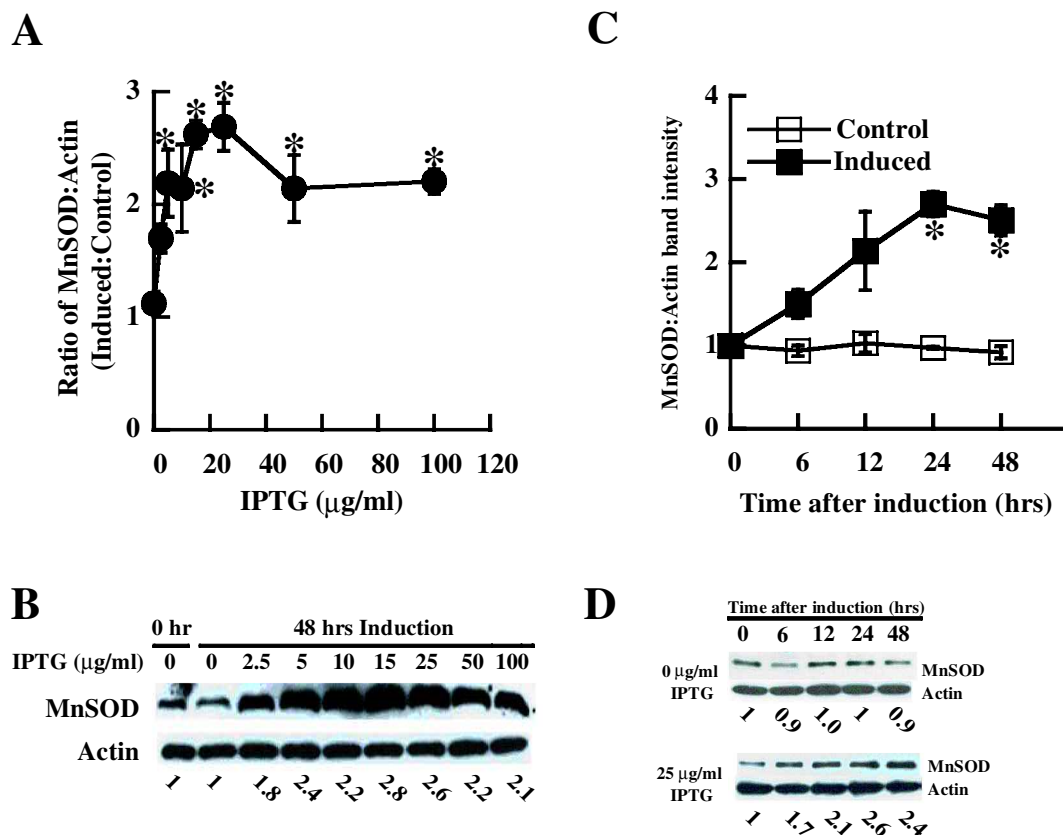


FIG. 1. Induction of immunoreactive MnSOD protein. (A) Immunoreactive MnSOD protein was induced in an IPTG dose-dependent manner. Cells were treated with various concentrations of IPTG for 48 h. Immunoreactive MnSOD protein was analyzed by western blot and quantified by densitometry. Values are means \pm SD ($n = 3$). * $p < 0.05$ compared with control at 0 h. (B) A western blot image from A with representative quantified values of MnSOD/actin below western blot. (C) Immunoreactive MnSOD protein was induced in an induction time-dependent manner. Cells were treated without (□) or with 25 $\mu\text{g}/\text{ml}$ IPTG (■) for a given time period. Immunoreactive MnSOD protein was analyzed by western blot and quantified by densitometry. Values are means \pm SD ($n = 3$). * $p < 0.05$ compared with control at 0 h. (D) Western blot images from C with representative quantified values of MnSOD/actin below western blot.

in the expression of MnSOD protein when the concentrations of IPTG were $>50 \mu\text{g/ml}$ IPTG, although elevated MnSOD levels compared with the control were maintained. This saturated expression pattern of MnSOD protein was also shown in the time-course study. With $25 \mu\text{g/ml}$ IPTG treatment, the maximum expression of MnSOD protein was achieved at 24 h after induction with a slight decrease at 48 h: 2.7-fold increase at 24 h versus 2.5-fold increase at 48 h (Fig. 1C and D). We hypothesize that down-regulation of endogenous MnSOD expression may occur at transcriptional and translational levels following expression of exogenous MnSOD protein. In inducible MnSOD-expressing clones developed from MDCK cells in a similar manner, the expression of endogenous canine MnSOD protein with slightly lower molecular weight than human MnSOD was decreased with increased human MnSOD expression after induction (data not shown), providing evidence to support this hypothesis. These observations are currently under further investigation in our laboratory to verify possible negative feedback regulation of MnSOD expression.

As hms1-clone cells were generated across species where host cells were mouse cells and the exogenous cDNA was of human origin, we verified the proper targeting of induced human MnSOD protein to mitochondria using immunogold EM. As shown in Fig. 2A, induced MnSOD protein was almost exclusively localized in mitochondria. No significant morphological change in mitochondria was observed after MnSOD induction (data not shown). A 2.3-fold increase in the number of gold beads per square micrometer of mitochondrial area after induction with $10 \mu\text{g/ml}$ IPTG for 48 h (Fig. 2B) was in good agreement with a 2.2-fold increase in MnSOD immunoreactive protein level determined by western blot analysis as demonstrated in Fig. 1A. Also, biochemical assay demonstrated that induced MnSOD immunoreactive protein was enzymatically active (Fig. 2C). After 48 h of induction with $25 \mu\text{g/ml}$ IPTG, there was a 2.2-fold increase in MnSOD activity measured by NBT-based biochemical assay. Immunogold EM showed that MnSOD protein increased in mitochondria as early as 3 h after initiation of induction (Fig. 2B). Although not statistically significant at 3 h, we believe

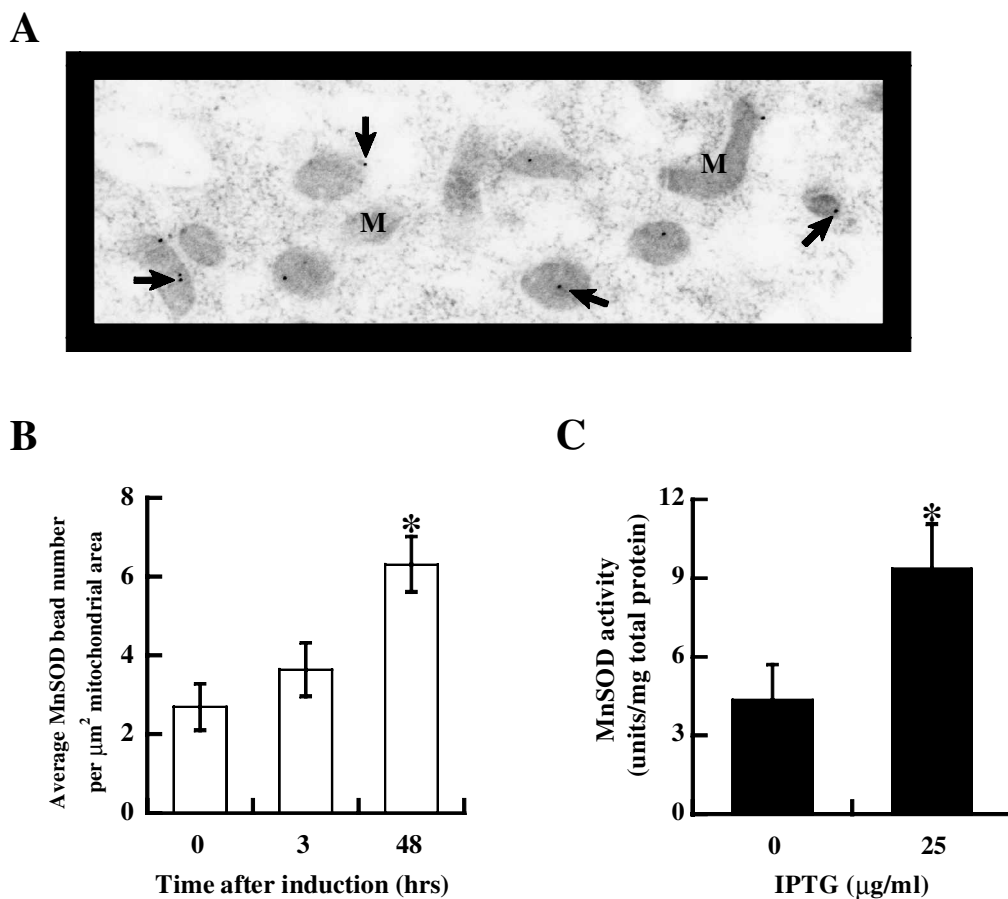


FIG. 2. Induced MnSOD protein is functional. (A) Representative immunogold EM image. MnSOD was induced with $10 \mu\text{g/ml}$ IPTG for 48 h. M, mitochondrion; arrow, immunogold bead directed against MnSOD protein; magnification: $\times 12,300$. (B) Human MnSOD protein was correctly targeted to mitochondria. MnSOD protein was induced with $10 \mu\text{g/ml}$ IPTG for 3 h or 48 h. Immunogold EM using primary antibody against MnSOD protein and quantitative image analysis were performed as described in Materials and Methods. Values are means \pm SEM ($n = 30$). $*p < 0.05$ compared with control at 0 h. (C) Induced human MnSOD protein was functional. Cells were treated with $25 \mu\text{g/ml}$ IPTG for 48 h. MnSOD activity was measured using NBT-based biochemical assay. Values are means \pm SD ($n = 3$). $*p < 0.05$ compared with control at 48 h.

this early increase in MnSOD has a biologically significant function as shown in our further studies described below.

Growth inhibition by induced MnSOD

Although it has been demonstrated that MnSOD levels are inversely correlated with cell growth (20), the method of choice in increasing MnSOD level was usually a constitutive gene expression system. These previous studies demonstrated that there were often cellular adaptations to constitutively overexpressed MnSOD (15–17). In our current study, we were able to demonstrate that decreased cellular growth was the direct outcome of increased MnSOD levels, not a reflection of adapted cellular phenotypes to elevated MnSOD levels. We induced MnSOD protein with 25 $\mu\text{g/ml}$ IPTG in exponentially proliferating cells, which was achieved at 48 h after initial seeding using our experimental conditions. A decrease in cell growth was shown as early as 24 h after initiation of induction, and growth inhibition of 32% and 30% compared with control cells was measured at 48 h and 72 h, respectively, after initiation of induction (Fig. 3). Neither hypodiploid nor hyperdiploid peaks were detected as defined by PI DNA profile in both control and MnSOD-induced cells with 25 $\mu\text{g/ml}$ IPTG up to 96 h, suggesting that neither apoptosis nor cell cycle block was present (data not shown).

As shown in Table 1, after 24 h of induction, the population doubling time (T_d) in MnSOD-overexpressing cells was ~ 8 h greater than that in control cells, whereas T_d values were not significantly different at 72 h after initiation of induction. Therefore, given sufficient time, exponentially proliferating cells with increased MnSOD levels resumed normal growth. In addition, when induction was initiated during the lag phase of the growth curve (at day 0 of Fig. 3), proliferation of MnSOD-induced cells was similar to that of the control (data not shown). The difference in T_d values at 96 h shown in Table 1 was due to different growth confluency in each condition; control cells reached the population density at which contact inhibition occurred, whereas induced cells did not quite reach such a critical density at 96 h. Thus, T_d of control was greater than that of MnSOD-overexpressing cells at 96 h after initia-

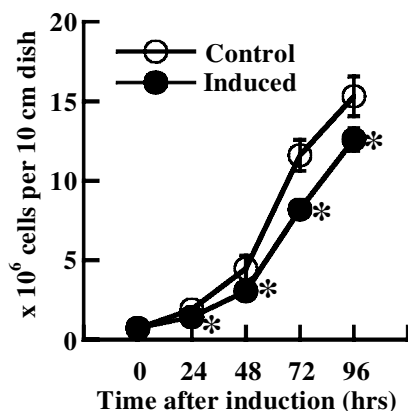


FIG. 3. Cell growth inhibition by overexpressed MnSOD. Cells were plated at 2×10^5 cells per 10-cm dish. When cells reached log phase, MnSOD was induced with 25 $\mu\text{g/ml}$ IPTG. Every 24 h, cells were counted using a Coulter counter. \circ , control cells; \bullet , 25 $\mu\text{g/ml}$ IPTG-treated cells. Values are means \pm SD ($n = 3$). * $p < 0.05$ compared with control at a given time point.

TABLE 1. INCREASED POPULATION DOUBLING TIME BY OVEREXPRESSED MnSOD

Time after induction	Doubling time (h)	
	Control condition	Induced condition
0 h	22.8 \pm 0.7	22.8 \pm 0.7
24 h	17.7 \pm 1.4	25.7 \pm 5.6*
48 h	20.2 \pm 4.0	22.8 \pm 4.4*
72 h	18.0 \pm 4.2	17.0 \pm 2.0
96 h	64.7 \pm 9.0	38.7 \pm 2.7*

Population doubling times (T_d) were calculated from the growth curves as shown in Fig. 3. Values are means \pm SD ($n = 3$).

* $p < 0.05$ compared with the control at a given time point.

tion of induction. Taken together, we hypothesized that rapid changes in MnSOD levels, not prolonged elevation of MnSOD activity, were physiologically significant for growth modulation by MnSOD.

Modulation of cell cycle kinetics by induced MnSOD

The estimation of cell cycle transition times using bivariate thymidine analogue cytometry is based on the relative movement of BrdU-incorporated cells compared with BrdU-negative cells within the completion of one cell cycle (31). With this approach, one can measure not only changes in potential doubling time (T_{pot}), but also cell cycle transition times of each cell cycle phase. As shown in Table 2, T_{pot} was significantly increased at 6 h after initiation of induction due to elevated T_{G1} and T_S cell cycle phases; an increase in T_{pot} was maintained up to 24 h. Similar to results from growth curves and T_d values, cells with prolonged MnSOD overexpression at 48 h had shorter T_{pot} than cells at 24 h after initiation of induction. The times described above were times of IPTG induction; actual total times for analysis of cell cycle transition times were 5.5 h longer due to the BrdU pulse and chase period. Our results demonstrated the resumption of normal cell cycle transition times in cells with a sustained increase in MnSOD levels.

Elevated MnSOD activity significantly delayed G_1 and S phase progressions (Table 2). None of the IPTG doses and induction times studied resulted in cell cycle block as defined by changes in PI DNA profile; also, the immunoreactive protein levels of cyclins (cyclins A, D, and E) and cyclin-dependent kinase inhibitors (p15/INK4B, p16/INK4A, p21/WAF1/CIP1, p27/KIP1) were not changed when measured by western blotting (data not shown). Statistically significant changes in G_1 and S phase transition times were observable as early as 6 h after initiation of induction, suggesting very rapid cellular response to elevation of MnSOD levels. To confirm this further, we sorted cells in G_1 phase and monitored cell cycle progression of sorted cells. As shown in Fig. 4, 40% of control cells progressed into S phase, whereas only 33% of cells with elevated MnSOD level induced by 25 $\mu\text{g/ml}$ IPTG did so at 12 h after replating. Together, these findings indicate moderate, but fast modulation of cell cycle progression by MnSOD overexpression.

TABLE 2. CELL CYCLE KINETIC CHANGES BY OVEREXPRESSED MnSOD

Induction time (h)	Cell cycle transition time (h)			
	T_{pot}	T_{G1}	T_S	$T_{G2/M}$
0 h	16.6 ± 1.7	5.9 ± 1.2	8.0 ± 0.9	2.7 ± 0.4
6 h	20.7 ± 1.6*	8.3 ± 0.8*	9.8 ± 0.9*	2.6 ± 0.1
24 h	23.4 ± 1.6*	10.1 ± 1.3*	10.9 ± 0.8*	2.4 ± 0.2
48 h	19.2 ± 1.6†	7.4 ± 0.9†	9.2 ± 0.6†	2.5 ± 0.2

Cells were seeded at 2×10^5 per 10-cm dish and cultured for 48 h. MnSOD was induced with 25 μ g/ml IPTG for a given time period. Cell cycle transition times were measured using the relative movement of BrdU pulsed cells. Analysis of cell cycle transition times was performed 5.5 h after a given MnSOD induction time due to the BrdU pulse and chase period. T_{pot} , T_S , and $T_{G2/M}$ were calculated according to equations described previously (31); T_{G1} was calculated by subtracting T_S and $T_{G2/M}$ from T_{pot} . Values are means \pm SD ($n = 3$).

* $p < 0.05$ compared with control at 0 h.

† $p < 0.05$ compared with 24 h induced cells.

Reversible cell cycle regulation by induced MnSOD

If cell cycle modulation by MnSOD is physiological, changes in cell cycle kinetics should be reversible with the cessation of MnSOD induction. To test this, cells were cultured without or with 25 μ g/ml IPTG for 48 h and replated in various conditions: control cells were replated either without (culture condition A) or with 25 μ g/ml IPTG (culture condition B); MnSOD-induced cells with 25 μ g/ml IPTG for 48 h were replated in either the absence (culture condition C) or the presence of 25 μ g/ml IPTG (culture condition D). Upon withdrawal of IPTG for 48 h, the level of immunoreactive MnSOD protein was significantly decreased (compare C with D in Fig. 5A and lane 5 with lane 6 in Fig. 5B). As shown in Table 3, MnSOD

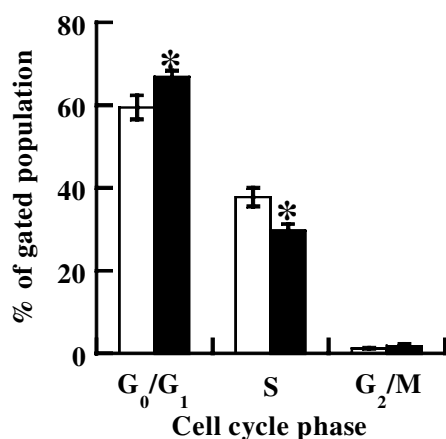


FIG. 4. G_1 phase progression is under the direct influence of MnSOD expression level. Cells in G_1 phase of the cell cycle were sorted and seeded as described in Materials and Methods. The progression of G_1 population within 12 h after replating in either the absence or the presence of 25 μ g/ml IPTG was measured using BrdU incorporation. Cell cycle profiles are shown as a percentage of gated population. Open columns, control cells; filled columns, 25 μ g/ml IPTG-treated cells. Values are means \pm SD ($n = 3$). * $p < 0.05$ compared with control.

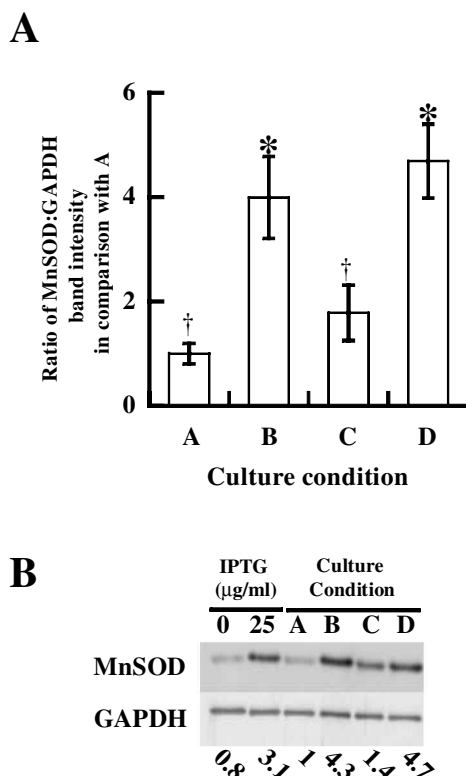


FIG. 5. MnSOD expression is reversible. (A) MnSOD was induced with 25 μ g/ml IPTG for 48 h. Cells were replated at 5×10^5 cells per 10-cm dish in various culture conditions. After 48 h, cells were collected for western blotting. Culture condition A: control before and after replating; culture condition B: control before replating and 25 μ g/ml IPTG treatment after replating; culture condition C: 25 μ g/ml IPTG treatment before replating and control after replating; culture condition D: 25 μ g/ml IPTG treatment before and after replating. Values are means \pm SD ($n = 3$). * $p < 0.05$ compared with culture condition A; † $p < 0.05$ compared with culture condition D. (B) Representative western blot images from A with quantified values of MnSOD/GAPDH below western blot.

TABLE 3. REVERSIBLE CELL CYCLE KINETIC CHANGES

Cell cycle transition time (h)	Culture condition			
	A	B	C	D
T_{pot}	22.4 ± 0.9	28.7 ± 0.4*	22.1 ± 0.6	27.4 ± 1.2*

Cells were treated as described in Fig. 5. Cell cycle kinetic changes were measured as described in Table 2. Values are means ± SD ($n = 3$).

* $p < 0.05$ compared with culture condition A.

levels in various conditions were directly correlated with their T_{pot} values. Importantly, condition C showed a 20% decrease in T_{pot} compared with condition D, and this was mainly due to shorter T_{G_1} (data not shown). These results demonstrated that changes in cell cycle kinetics were tightly linked to MnSOD levels and that growth inhibition by MnSOD was reversible.

Modulation of intracellular ROS levels by induced MnSOD

In other studies using constitutive gene expression systems to overexpress MnSOD in various cell types, elevated steady-state levels of intracellular ROS were documented (15–17, 25). We examined whether overexpressed MnSOD by an inducible gene expression system also increases intracellular ROS levels. We analyzed intracellular ROS levels in hms1-clone cells using the redox-sensitive H_2DCFDA dye and flow cytometry. As shown in Fig. 6A, a maximum of 30% increase in ROS levels over control was detected with 25 $\mu\text{g/ml}$ IPTG treatment. A peak level of ROS was observed at 3 h after initiation of induction with a significant decrease at 6 h. Steady-state levels of ROS were ~50% of the control. A transient decrease in mitochondrial membrane potential at 3 h after initiation of induction was also detected.

Changes in the steady-state levels of ROS were reversible and tightly associated with the levels of MnSOD. As shown in Fig. 6B, upon withdrawal of IPTG for 48 h, the levels of ROS were significantly increased (compare culture condition C with D) and became similar to the control level (compare culture condition C with A). However, there was no significant difference in mitochondrial membrane potentials among various culture conditions (data not shown). From these results, we concluded that unlike results reported by other studies using constitutive MnSOD expression systems (15–17, 25), a very rapid and transient increase in ROS levels was correlated with regulation of cell cycle progression by MnSOD and that sustained ROS elevation was not required for growth inhibition.

N-Acetyl-L-cysteine (NAC) blocks growth inhibition by induced MnSOD

NAC is one of the most frequently used antioxidants in short-term cell culture studies. However, prolonged exposure to NAC can either selectively delay G_0/G_1 phase transition (18) or result in biphasic changes in cell growth, viability, and apoptosis depending on NAC concentrations (7). We tested dose-response patterns of growth of hms1-clone cells at various doses of NAC following 48 h of treatment. Dramatic de-

creases in cellular proliferation were observed with NAC concentrations between 100 μM and 1 mM , whereas concentrations of 5 mM to 10 mM resulted in indistinguishable cell growth from control. However, even higher concentrations of NAC led to decreases in viability (data not shown). Therefore, we chose 5 mM NAC to determine the effect of modulation of cellular redox states after 3 h of induction on growth inhibition by MnSOD. As shown in Fig. 6C, a 30% decrease in cell growth following MnSOD induction for 48 h by 25 $\mu\text{g/ml}$ IPTG was reversed to the control level with 5 mM NAC treatment. Therefore, 5 mM NAC treatment had no effect on cell growth, but blocked the cell growth inhibition caused by overexpression of MnSOD.

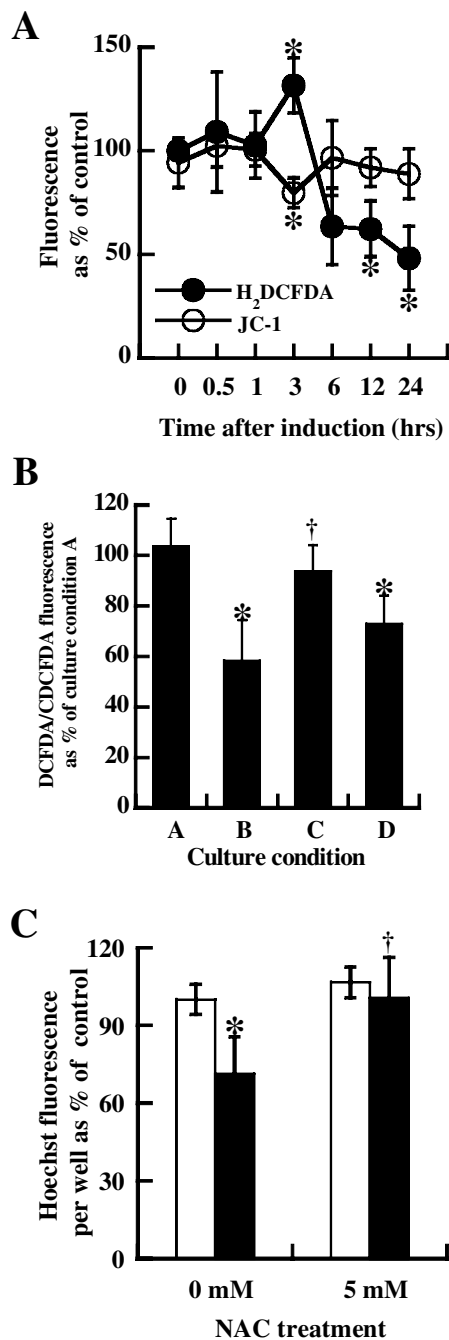
DISCUSSION

Cellular redox state and intracellular ROS, which are still often very qualitatively described due to the technical challenges involved in quantification (26), are known to regulate many cellular processes, including proliferation, differentiation, apoptosis, and necrosis. Cellular redox states and ROS levels are often perceived as passively modulating cellular characteristics secondary to oxidative stress and oxidative damage; however, cellular redox state and ROS are now known to be mechanisms by which cells actively regulate their physiology. Therefore, cells must be able to modulate cellular redox state and ROS in a tightly controlled and precise manner to maintain optimal cell physiology.

The growth inhibitory function of MnSOD is an unusual property of an AOE. Although CuZnSOD catalyzes the same enzymatic reaction as MnSOD, overexpression of CuZnSOD using stable transfection technique has not shown strong correlation with cell growth in murine fibroblasts (9, 10). It has been suggested that production of H_2O_2 by MnSOD is the cause of cell growth inhibition. However, this conclusion is based on results from constitutive gene expression systems in which adaptation is known to be prominent, making analysis of data more difficult (15–17, 25). The present study confirms and extends the observations from previous studies by using an inducible gene expression system in which adaptation does not occur, and determines for the first time that cell growth inhibition is due to a delay in cell cycle progression.

Similar observations to those demonstrated in the current study were made in our laboratory when MnSOD was overexpressed using an adenoviral vector system (11). In this system, increased ROS levels generated by MnSOD overexpression were correlated with delays in G_1 and S phase transition times in a MnSOD gene dose-dependent manner; in addition,

FIG. 6. Cellular redox modulation is involved in growth inhibition by MnSOD. (A) At time 0 h, MnSOD was induced with 25 $\mu\text{g}/\text{ml}$ IPTG. Intracellular ROS and mitochondrial membrane potential were measured at various time points using redox-sensitive H_2DCFDA dye and JC-1 dye, respectively. At a given time, fluorescence was expressed as a percentage of control. ●, H_2DCFDA ; ○, JC-1. Values are means \pm SD ($n = 5$). * $p < 0.05$ compared with control at 0 h. (B) Cells were treated as described in Fig. 5 and stained with H_2DCFDA and CDCFDA as described in Materials and Methods. Fluorescence of H_2DCFDA was normalized over CDCFDA and expressed as a percentage of culture condition A. Values are means \pm SD ($n = 5$). * $p < 0.05$ compared with culture condition A; † $p < 0.05$ compared with culture condition D. (C) Cells were seeded at 3,000 cells per well in 96-well plates. Twenty-four hours later, MnSOD was induced with 25 $\mu\text{g}/\text{ml}$ IPTG in the absence or presence of 5 mM NAC. Cellular proliferation at 48 h after initiation of induction was measured using Hoechst fluorescence as described in Materials and Methods. Hoechst fluorescence was expressed as a percentage of control without NAC treatment. Open columns, for control condition; filled columns, induced condition. Values are means \pm SD ($n = 6$). * $p < 0.05$ compared with control without 5 mM NAC treatment; † $p < 0.05$ compared with induced condition without 5 mM NAC treatment.



prolonged overexpression of MnSOD led to spontaneous apoptosis. Although we observed significantly impaired mitochondrial membrane potential, decreased ATP content, and reduced ratio of glutathione (GSH) to glutathione disulfide (GSSG), these changes were associated only with apoptotic events, not with delays in cell cycle transition times. Herein, we propose that SODs are AOEes because they eliminate $\text{O}_2^{\cdot-}$; however, they also have prooxidant activity because they produce H_2O_2 .

When MnSOD was constitutively overexpressed in malignant as well as nonmalignant cells, clones selected for studies often had an adapted phenotype of altered AOE profiles, ex-

amples being decreased CuZnSOD activity and increased catalase or GPx activity. The former change has been proposed to represent an effort to reduce the production of H_2O_2 , whereas the latter two alterations increase H_2O_2 -removing capacity. ROS levels were directly correlated with growth inhibition in clones from both NIH/3T3 fibroblasts and DU145 prostate carcinoma cells following constitutive overexpression of MnSOD (15–17).

When H_2O_2 production is sufficiently elevated by increased MnSOD activity, it could directly inhibit Krebs cycle enzymes (19) or respiratory chain functions (25). H_2O_2 could also diffuse out of mitochondria, and other cellular compart-

ments would then be subjected to oxidative stress. However, when MnSOD was inducibly overexpressed, we failed to detect either cell cycle blocks (data not shown) or changes in levels of cyclins and/or cyclin-dependent kinase inhibitors that are often associated with growth inhibition by exogenous H_2O_2 treatments. These observations suggest that oxidative stress in the cytoplasm and/or nucleus is low and that alternative mechanisms are used for the modulation of cell cycle kinetics by inducibly overexpressed MnSOD. As the involvement of phosphorylated cyclins in cell cycle regulation has been demonstrated (1, 13), further studies are required to determine whether changes in cell cycle kinetics by inducibly overexpressed MnSOD are determined by modulation of the levels of phosphorylated cyclins.

The results from the current study using an inducible MnSOD expression system support the concept that the prooxidant activity of MnSOD is responsible for cell growth inhibition. Causative roles of transient ROS increase on decreased mitochondrial membrane potential and cell cycle regulation were strongly suggested from the time-course studies of these variables; alteration of ROS levels preceded changes in cell cycle kinetics (compare Table 2 and Fig. 6A). Mitochondrial membrane potential was decreased only when ROS levels were elevated above control (Fig. 6A). An increase in ROS at 3 h after initiation of induction was coincident with elevated immunoreactive MnSOD protein in mitochondria as demonstrated using immunogold EM, although western blotting analysis with whole-cell homogenates failed to detect change in MnSOD protein at 3 h after initiation of induction. We have demonstrated in our laboratory that the immunogold EM technique is more sensitive than western blotting for detection of immunoreactive MnSOD protein (unpublished observations). A decrease in ROS at 6 h after initiation of induction is speculated to be due to an adaptive response of mitochondria to elevated ROS levels, although mechanisms utilized by mitochondria to accomplish this are currently unclear.

There were no significant changes in ATP content, total GSH content, ratio of GSH to GSSG, or CuZnSOD and GPx activities upon MnSOD induction in hms1-clone cells (data not shown). These observations from inducible MnSOD overexpression were not readily explainable by current hypotheses developed from studies using constitutive gene expression systems, in which the above-mentioned biochemical parameters were often modulated in MnSOD-overexpressing cells. In current studies, when produced at low levels, H_2O_2 seems to serve as a physiological ROS and a signaling molecule, not as a harmful oxidant. This may explain the transient increase in ROS levels; it was potent enough to impair temporarily the mitochondrial membrane potential, but not sufficient enough to interfere with mitochondrial function such as ATP generation. ROS were rapidly, but transiently produced in cells as a response to increased MnSOD activity; a physiological consequence of MnSOD overexpression was a temporary delay in cell cycle progression. Our results have a precedent in the mechanism by which plasma membrane signaling cascades (*e.g.*, growth factor-driven) utilize ROS as signaling molecules (3).

As all mitochondrial antioxidants and AOE are produced in the cytoplasm and delivered into mitochondria in a controlled and precise fashion, in the long term, mitochondrial

redox state is at least partially an extension of cytoplasmic redox environment. However, mitochondrial redox state is independently regulated in the short term as a result of cellular compartmentalization. For example, mitochondria often have higher concentrations of GSH than other subcellular compartments (26), and depletion of GSH in other compartments is not directly reflected in mitochondrial GSH levels (28). Therefore, changes in mitochondrial ROS levels will strongly affect the mitochondrial redox environment. Studies to clarify the effects of modulation of mitochondrial redox on other subcellular compartments are currently in progress in our laboratory.

The expression of endogenous MnSOD is tightly correlated with cellular proliferation. Quiescent or confluent cells have increased MnSOD activity compared with exponentially proliferating cells (21, 22). MnSOD activity is also further regulated in a cell cycle-dependent manner with the lowest MnSOD activity during S phase in NIH/3T3 mouse embryo fibroblasts and human DU145 prostate carcinoma cells (22). Taken together, we postulate that cells may actively modulate MnSOD activity in such a manner that they can finely regulate cell cycle progression, perhaps by alteration of mitochondrial redox state, without involving dramatic changes in levels of cell cycle regulatory proteins.

In our current study, we demonstrated that increased MnSOD activity led to a transient increase in ROS and concomitant decrease in mitochondrial membrane potential. The prooxidant activity of MnSOD may lead to these changes. Changes in cell cycle progression were correlated with these initial changes. Population doubling time was increased, and G_1 and S phase progressions were delayed. However, cell cycle kinetic modulation by MnSOD was temporary and reversible. Taken together, we hypothesize that a major role of MnSOD is not only to protect mitochondria against $O_2^{\cdot-}$, but also to coordinate mitochondrial function and cell proliferation. The availability of H_2O_2 will be determined by mitochondrial redox state; impaired mitochondrial redox capacity prolongs the availability of H_2O_2 and leads to decreased cellular proliferation. Our current hypothesis is unique and novel in that cells utilize a prooxidant activity of an AOE to coordinate biochemical activities in different subcellular compartments. Further studies are required to test this hypothesis.

ACKNOWLEDGMENTS

We thank Drs. Igor B. Roninson and Bey-Dih Chang (The University of Illinois, Chicago, IL, U.S.A.) for generous gifts of 3' SS1 cells, LNXCO3, and other retroviral vectors. We also thank Dr. Larry W. Oberley (The University of Iowa, Iowa City, IA, U.S.A.) for providing us with human MnSOD cDNA and antibody against human MnSOD. Excellent suggestions by Dr. Larry W. Oberley during the course of the current study are deeply appreciated by the authors. We thank Mrs. Kathleen Schell at the flow cytometry facility at the UW Comprehensive Cancer Center for technical support (grant CA14520-29). This work was supported by the Office of Research and Development, Medical Research Service, Department of Veterans Affairs.

ABBREVIATIONS

AOE, antioxidant enzyme; ARE, antioxidant response element; BrdU, bromodeoxyuridine; CDCFDA, 5-(and-6)-carboxy-2',7'-dichlorofluoresceindiacetate; CuZnSOD, copper- and zinc-containing superoxide dismutase; DMEM, Dulbecco's modified Eagle medium; ECSOD, extracellular CuZnSOD; EM, electron microscopy; GAPDH, glyceraldehyde-3-phosphate dehydrogenase; GPx, glutathione peroxidase; GSH, glutathione; GSSG, glutathione disulfide; H₂DCFDA, 2',7'-dichlorofluorescein diacetate; hms1-clone, a cell line developed from NIH/3T3 mouse fibroblasts that inducibly overexpresses human MnSOD protein; H₂O₂, hydrogen peroxide; IPTG, isopropyl β-thiogalactoside; JC-1, 5,5',6,6'-tetrachloro-1,1',3,3'-tetraethylbenzimidazolyl carbocyanine iodide; KR buffer, Krebs-Ringer buffer; MDCK, canine normal kidney epithelial cell line; MnSOD, manganese-containing superoxide dismutase protein; NAC, N-acetyl-L-cysteine; NBT, nitro blue tetrazolium; O₂⁻, superoxide anion; PBS, phosphate-buffered saline; PI, propidium iodide; ROS, reactive oxygen species; SOD, superoxide dismutase; *sod2*, MnSOD gene; T_d, population doubling time; T_{G1}, G₁ phase transition time; T_{G2/M}, G₂/M phase transition time; T_{pot}, potential doubling time; T_S, S phase transition time.

REFERENCES

- Alt JR, Gladden AB, and Diehl JA. p21^{Cip1} promotes cyclin D1 nuclear accumulation via direct inhibition of nuclear export. *J Biol Chem* 277: 8517–8523, 2002.
- Arnold RS, Shi J, Murad E, Whalen AM, Sun CQ, Polavarapu R, Parthasarathy S, Petros JA, and Lambeth JD. Hydrogen peroxide mediates the cell growth and transformation caused by the mitogenic oxidase Nox1. *Proc Natl Acad Sci U S A* 98: 5550–5555, 2001.
- Bedogni B, Pani G, Colavitti R, Riccio A, Borrello S, Murphy M, Smith R, Eboli ML, and Galeotti T. Redox regulation of cAMP-responsive element-binding protein and induction of manganese superoxide dismutase in nerve growth factor-dependent cell survival. *J Biol Chem* 278: 16510–16519, 2003.
- Buettner GR. The pecking order of free radicals and antioxidants: lipid peroxidation, α-tocopherol, and ascorbate. *Arch Biochem Biophys* 300: 535–543, 1993.
- Chang B and Roninson IB. Inducible retroviral vectors regulated by *lac* repressor in mammalian cells. *Gene* 183: 137–142, 1996.
- Copin JC, Gasche Y, and Chan PH. Overexpression of copper/zinc superoxide dismutase does not prevent neonatal lethality in mutant mice that lack manganese superoxide dismutase. *Free Radic Biol Med* 28: 1571–1576, 2000.
- Hernandez-Saavedra D and McCord JM. Paradoxical effects of thiol reagents on Jurkat cells and a new thiol-sensitive mutant form of human mitochondrial superoxide dismutase. *Cancer Res* 63: 159–163, 2003.
- Jones PL, Ping D, and Boss JM. Tumor necrosis factor alpha and interleukin-β regulate the murine manganese superoxide dismutase gene through a complex intronic enhancer involving C/EBP-β and NF-κB. *Mol Cell Biol* 17: 6970–6981, 1997.
- Kelner MJ and Bagnell R. Alteration of endogenous glutathione peroxidase, manganese superoxide dismutase, and glutathione transferase activity in cells transfected with a copper-zinc superoxide dismutase expression vector. *J Biol Chem* 265: 10872–10875, 1990.
- Kelner MJ, Bagnell R, Montoya M, Estes L, Uglik SF, and Cerutti P. Transfection with human copper-zinc superoxide dismutase induces bidirectional alterations in other antioxidant enzymes, proteins, growth factor response, and paraquat resistance. *Free Radic Biol Med* 18: 497–506, 1995.
- Kim A, Oberley LW, and Oberley TD. Growth inhibition by overexpressed MnSOD in human fibroblasts. 9th Annual Meeting of The Oxygen Society, abstract number 314, 2002.
- Kops GJPL, Dansen TB, Polderman PE, Saarloos I, Wirtz KWA, Coffey PJ, Huang T, Bos JL, Medema RH, and Burgering BMT. Forkhead transcription factor FOXO3a protects quiescent cells from oxidative stress. *Nature* 419: 316–321, 2002.
- Lenferink AEG, Busse D, Flanagan WM, Yakes M, and Arteaga CL. ErbB2/*neu* kinase modulates cellular p27^{Kip1} and cyclin D1 through multiple signaling pathways. *Cancer Res* 61: 6583–6591, 2001.
- Lewis M, Chang G, Horton NC, Kercher MA, Pace HC, Schumacher MA, Brennan RG, and Lu P. Crystal structure of the lactose operon repressor and its complexes with DNA and inducer. *Science* 271: 1247–1254, 1996.
- Li N, Oberley TD, Oberley LW, and Zhong W. Inhibition of cell growth in NIH/3T3 fibroblasts by overexpression of manganese superoxide dismutase: mechanistic studies. *J Cell Physiol* 175: 359–369, 1998.
- Li N, Oberley TD, Oberley LW, and Zhong W. Overexpression of manganese superoxide dismutase in DU145 human prostate carcinoma cells has multiple effects on cell phenotype. *Prostate* 35: 221–233, 1998.
- Li N, Zhai Y, and Oberley TD. Two distinct mechanisms for inhibition of cell growth in human prostate carcinoma cells with antioxidant enzyme imbalance. *Free Radic Biol Med* 26: 1554–1568, 1999.
- Menon SG, Sarsour EH, Spitz DR, Higashikubo R, Sturm M, Zhang H, and Goswami P. Redox regulation of the G₁ to S phase transition in the mouse embryo fibroblast cell cycle. *Cancer Res* 63: 2109–2117, 2003.
- Nulton-Persson AC and Szewda LI. Modulation of mitochondrial function by hydrogen peroxide. *J Biol Chem* 276: 23357–23361, 2001.
- Oberley LW. Anticancer therapy by overexpression of superoxide dismutase. *Antioxid Redox Signal* 3: 461–472, 2001.
- Oberley TD, Schultz JL, and Oberley LW. In vitro modulation of antioxidant enzyme levels in normal hamster kidney and estrogen-induced hamster kidney tumor. *Free Radic Biol Med* 16: 741–751, 1994.
- Oberley TD, Schultz JL, Li N, and Oberley LW. Antioxidant enzyme levels as a function of growth state in cell culture. *Free Radic Biol Med* 19: 53–65, 1995.
- Oberley TD, Xue Y, Zhao Y, Kinningham K, Szewda LI, and St. Clair DK. *In situ* reduction of oxidative damage, increased cell turnover, and delay of mitochondrial injury by

- overexpression of manganese superoxide dismutase in a multistage skin carcinogenesis model. *Antioxid Redox Signal* 6: 537–548, 2004.
24. Rago R, Mitchen J, and Wilding G. DNA fluorometric assay in 96-well tissue culture plates using Hoechst 33258 after cell lysis by freezing in distilled water. *Anal Biochem* 191: 31–34, 1990.
 25. Rodríguez AM, Carrico PM, Mazurkiewicz JE, and Meléndez JA. Mitochondrial or cytosolic catalase reverses the MnSOD-dependent inhibition of proliferation by enhancing respiratory chain activity, net ATP production, and decreasing the steady state levels of H₂O₂. *Free Radic Biol Med* 29: 801–813, 2000.
 26. Schafer FQ and Buettner GR. Redox environment of the cell as viewed through the redox state of the glutathione disulfide/glutathione couple. *Free Radic Biol Med* 30: 1191–1212, 2001.
 27. Serra V, von Zglinicki T, Lorenz M, and Saretzki G. Extracellular superoxide dismutase is a major antioxidant in human fibroblasts and slows telomere shortening. *J Biol Chem* 278: 6824–6830, 2003.
 28. Seyfried J, Soldner F, Schulz JB, Klockgether T, Kovar KA, and Wüllner U. Differential effects of L-buthionine sulfoximine and ethacrynic acid on glutathione levels and mitochondrial function in PC12 cells. *Neurosci Lett* 264: 1–4, 1999.
 29. Takeuchi H, Kobayashi Y, Ishigaki S, Doyu M, and Sobue G. Mitochondrial localization of mutant superoxide dismutase 1 triggers caspase-dependent cell death in a cellular model of familial amyotrophic lateral sclerosis. *J Biol Chem* 277: 50966–50972, 2002.
 30. Thimmulappa RK, Mai KH, Srisuma S, Kensler TW, Yamamoto M, and Biswal S. Identification of Nrf2-regulated genes induced by the chemopreventive agent sulforaphane by oligonucleotide microarray. *Cancer Res* 62: 5196–5203, 2002.
 31. White RA, Meistrich ML, Pollack A, and Terry NHA. Simultaneous estimation of T_{G2+M}, T_S and T_{POT} using single sample dynamic tumor data from bivariate DNA-thymidine analogue cytometry. *Cytometry* 41: 1–8, 2000.
 32. Zhong HJ, Yan T, Oberley TD, and Oberley LW. Comparison of effects of two polymorphic variants of manganese superoxide dismutase on human breast MCF-7 cancer cell phenotype. *Cancer Res* 59: 6276–6283, 1999.

Address reprint requests to:

Terry D. Oberley

William S. Middleton Veterans Memorial Hospital, Room A35

2500 Overlook Terrace

Madison, WI 53705

E-mail: toberley@facstaff.wisc.edu

Received for publication October 7, 2003; accepted February 19, 2004.